FLORE
Repository istituzionale dell'Università degli Studi di Firenze

Exploring the biochemical mechanisms of cytotoxic gold compounds: a proteomic study.

Questa è la Versione finale referata (Post print/Accepted manuscript) della seguente pubblicazione:

Original Citation:

Exploring the biochemical mechanisms of cytotoxic gold compounds: a proteomic study / F. Magherini; A. Modesti; L. Bini; M. Puglia; I. Landini; S. Nobili; E. Mini; M.A. Cinellu; C. Gabbiani; L. Messori. - In: JBIC. - ISSN 0949-8257. - ELETTRONICO. - 15:(2010), pp. 573-582. [10.1007/s00775-010-0624-3]

Availability:

This version is available at: 2158/385773 since: 2017-07-17T15:18:46Z

Published version:

DOI: 10.1007/s00775-010-0624-3

Terms of use:

Open Access

La pubblicazione è resa disponibile sotto le norme e i termini della licenza di deposito, secondo quanto stabilito dalla Policy per l'accesso aperto dell'Università degli Studi di Firenze (https://www.sba.unifi.it/upload/policy-oa-2016-1.pdf)

Publisher copyright claim:

(Article begins on next page)

24 April 2024

J Biol Inorg Chem (2010) 15:573–582
DOI 10.1007/s00775-010-0624-3

ORIGINAL PAPER

Exploring the biochemical mechanisms of cytotoxic gold compounds: a proteomic study

Francesca Magherini · Alessandra Modesti · Luca Bini · Michele Puglia · Ida Landini · Stefania Nobili · Enrico Mini · Maria Agostina Cinellu · Chiara Gabbiani · Luigi Messori

Received: 23 October 2009 / Accepted: 28 December 2009 / Published online: 29 January 2010
© SBIC 2010

Abstract We have recently shown that a group of structurally diverse gold compounds are highly cytotoxic toward a panel of 36 human tumor cell lines through a variety of biochemical mechanisms. A classic proteomic approach is exploited here to gain deeper insight into those mechanisms. This investigation is focused on Auoxo6, a novel binuclear gold(III) complex, and auranofin, a clinically established gold(I) antiarthritic drug. First, the 72-h cytotoxicity profiles of Auoxo6 and auranofin were determined against A2780 human ovarian carcinoma cells. Subsequently, protein extraction from gold-treated A2780 cells sensitive to cisplatin and 2D gel electrophoresis separation were carried out according to established procedures. Notably, both metallodrugs caused relatively modest changes in protein expression in comparison with controls as only 11 out of approximately 1,300 monitored spots showed appreciable quantitative changes. Very remarkably, six altered proteins were in common between the two treatments. Eight altered proteins were identified by mass spectrometry; among them was ezrin, a protein associated with the cytoskeleton and involved in apoptosis. Interestingly, two altered proteins, i.e., peroxiredoxins 1 and 6, are known to play crucial roles in the cell redox metabolism. Increased cleavage of heterogeneous ribonucleoprotein H was also evidenced, consistent with caspase 3 activation. Overall, the results of the present proteomic study point out that the mode of action of Auoxo6 is strictly related to that of auranofin, that the induced changes in protein expression are limited and selective, that both gold compounds trigger caspase 3 activation and apoptosis, and that a few affected proteins are primarily involved in cell redox homeostasis.

Keywords Proteomic · Gold compound

F. Magherini · A. Modesti (✉)
Department of Biochemical Sciences,
University of Florence,
Viale G. Morgagni, 50,
50134 Florence, Italy
e-mail: modesti@scibio.unifi.it

L. Bini · M. Puglia
Department of Molecular Biology,
University of Siena,
Siena, Italy

I. Landini · S. Nobili · E. Mini
Department of Pharmacology,
University of Florence,
viale Pieraccini 6,
50139 Florence, Italy

M. A. Cinellu
Department of Chemistry,
University of Sassari,
Via Vienna 2,
07100 Sassari, Italy

C. Gabbiani · L. Messori (✉)
Department of Chemistry,
University of Florence,
via della Lastruccia 3,
50019 Sesto Fiorentino, Italy
e-mail: luigi.messori@unifi.it

Introduction

In the past few decades considerable efforts were made in the search of new metal-based anticancer agents that might display innovative mechanisms of action and, thus offer significant pharmacological advantages over the clinically established antitumor platinum drugs (i.e., cisplatin, carboplatin, and oxaliplatin). Accordingly, several new platinum and non-platinum compounds were prepared, characterized,

and evaluated as potential cytotoxic and antitumor drugs [1, 2].

In recent years research has increasingly focused on gold(III) compounds as anticancer drug candidates because gold(III) complexes typically display the same electronic configuration (d^8) and similar structural and reactivity features of platinum(II) complexes (in particular a strong preference for square-planar geometry and a rather favorable kinetic profile) [3]. Accordingly, our laboratories have developed a variety of structurally diverse gold(III) compounds as potential chemotherapeutic leads [4]. We previously reported that one of these complexes, namely, the binuclear gold(III) complex Auoxo6, manifests very encouraging cytotoxic properties in vitro and constitutes a new promising chemotherapeutic lead [5, 6].

In the present study we adopted a classic proteomic strategy to further investigate the mode of action of Auoxo6 in contrasting cancer cell growth. The behavior of Auoxo6 is compared with that of auranofin, a gold(I) antiarthritic drug, endowed with significant cytotoxic properties in vitro (but not in vivo) [7]. Auranofin was chosen as a control compound since it is a typical gold(I) drug in clinical use and a lot is known about its biochemical effects at the cellular level [8, 9]. The chemical structures of Auoxo6 and auranofin are shown in Fig. 1.

Previous studies showed that cytotoxic gold(III) compounds are able to induce cell death through apoptosis [10, 11]. However, for most gold compounds, apoptosis seems to be essentially triggered by direct mitochondrial damage, and is not the consequence of an initial DNA lesion, as in the case of cisplatin. Within this frame, the pivotal role of thioredoxin reductase as a probable target for cytotoxic gold compounds was highlighted [12]. In particular, it seems very likely that a strong inhibition of mitochondrial thioredoxin reductase may eventually lead to a deep alteration of the mitochondrial membrane potential, to release of cytochrome *c*, and to consequent triggering of apoptosis [12]. Such a type of "mitochondrial mechanism" was also proposed for gold(III) porphyrins [11], on which detailed proteomic studies were recently carried out, and for auranofin and a few related gold(I) compounds [13].

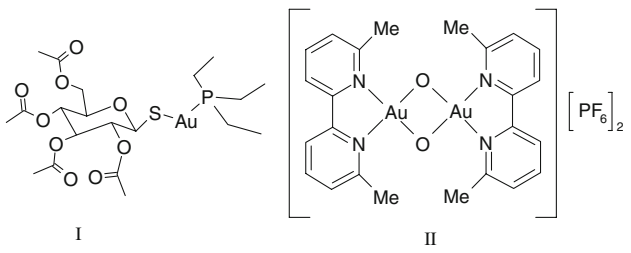

I II

Fig. 1 Auranofin (*I*) and Auoxo6 (*II*)

The relatively recent discipline of proteomics is mainly concerned with the analysis and the characterization of the protein products of the genome, known as the "proteome" [14, 15]. The aim of proteomics also includes the investigation of protein cellular activities and functions, and the analysis of the flow of information within the cell. A large part of this information is provided by several protein networks, organized in discrete signal transduction pathways, which control ultimately cell apoptosis. Proteomic profiling, therefore, offers a good opportunity to identify the proteins that mediate the apoptotic pathways when cells are treated with cytotoxic agents.

Notably, a few examples already exist in the literature where proteomic methods have been successfully utilized for investigating the mode of action of anticancer metallodrugs [16]. The mechanisms of action of anticancer metallodrugs are usually very complicate and variegate owing to the high reactivity of these compounds toward biomolecules, to their being (in most cases) *prodrugs* (thus undergoing large chemical transformations within the biological milieu), and to the large differences in electronic structure and reactivity existing among the various metal centers. The intrinsic high reactivity of metallodrugs typically leads to the occurrence of numerous interactions with a multitude of biomolecules, of which only a few are biochemically and functionally relevant. This situation may render the target identification and validation processes for metallodrugs very troublesome.

Some previous attempts to use classic proteomic methods to reveal the mechanism of action of metal-based cytotoxic drugs were carried out. In particular, the proteomic responses of cancer cells to platinum compounds were analyzed through a few studies. Yim et al. [17] examined differential protein expression in cisplatin-treated HeLa cervical carcinoma cells and found 21 altered proteins, of which 12 were upregulated and nine were downregulated. Notably, these authors showed that cisplatin induced a marked downregulation of nuclear factor κB; in addition, activation of both death-receptor-mediated and mitochondria-mediated apoptotic pathways was documented. Yao et al. [18] carried out comparative proteomic studies of colon cancer cells in response to oxaliplatin treatment and highlighted a number of proteins (around 20) that were simultaneously altered in three distinct colon cancer cell lines, namely, HT29, SW620, and LoVo. These overlapping proteins were identified and found to take part in many cellular processes, such as apoptosis, signal transduction, transcription and translation, cell structural organization, and metabolism. Notably, one of these altered proteins was ezrin. In turn, Che et al. [19] used 2D electrophoresis based proteomic technology to investigate the protein expression profiles of human nasopharyngeal carcinoma SUNE1 cells upon treatment with gold(III)

porphyrin 1a [20]. Relevant changes in the expression of a number of proteins engaged in redox metabolism, in the mitochondrial functions, and in apoptosis pathways were detected. In particular, voltage-dependent anion channel (VDAC) 1 was found to be highly upregulated. VDAC 1 is a mitochondrial outer-membrane channel protein which functions as a main pathway for the movement of various substances in and out of the mitochondria [21] and is considered to be a component of the permeability transition pore oligoprotein complex. These large alterations of VDAC expression suggested that mitochondria could be a primary target for gold(III) porphyrin 1a. Overall, the above-mentioned papers document the feasibility and the effectiveness of a classic proteomic approach.

Moreover, it is worth noting here that in the case of metallodrugs additional proteomic experiments may be devised that are centered on the metal and are principally aimed at investigating metal distribution patterns within the proteome (metallomics) [22–24]. These investigative approaches, relying on the selective tagging of the metallodrug or of the metal itself within 1D or 2D gels through highly sensitive methods, allow in principle the identification of all those proteins capable of binding the metallodrug of interest. Indeed, it is very likely that the effective targets for the metallodrug investigated are to be searched for among the proteins with which the metal is tightly associated. A few notable examples of this kind of strategy are available in the recent literature [25–28]. Nowadays, metallomic studies may take particular advantage of the use of very sensitive hyphenated methods as extensively documented by Becker et al. [29] and by other research groups in a few recent papers and reviews.

We report here the results of a classic proteomic study on the cellular effects of two prototypical cytotoxic gold compounds, i.e., Auoxo6 and auranofin. Upon comparing the proteomic profiles of A2780 cancer cells treated with Auoxo6 or auranofin with those of controls, we could identify a small number of differentially expressed proteins by mass spectrometry (MS). In turn, detailed functional analyses of the few altered proteins provide valuable insight into the possible biochemical mechanisms that are elicited by these two gold compounds, leading in both cases to apoptotic cancer cell death.

Materials and methods

Materials and reagents

Auoxo6 was synthesized as described in [30], and auranofin was purchased from Vinci Biochem. All other chemicals were of analytical grade. RPMI 1640 cell culture medium, fetal calf serum, and phosphate-buffered saline were purchased from Celbio (Milan, Italy); sulforhodamine B (SRB) was from Sigma (Milan, Italy).

Cell lines and cell culture

The cytotoxic properties of Auoxo6 and auranofin were analyzed in vitro according to the standard procedure described by Skehan et al. [31] working on the A2780 ovarian carcinoma human cell line either sensitive (A2780/S) or resistant (A2780/R) to cisplatin. This method estimates the residual cell number after drug treatment on the basis of quantitative determination of total cellular proteins after staining with SRB. Exponentially growing cells were inoculated into 96-well microtiter plates. After 24 h, the medium was removed and replaced with fresh medium containing an appropriate drug concentration for a continuous drug exposure of 72 h.

Then, cells were fixed in situ by 10% cold trichloroacetic acid and stained by SRB solution at 0.4% (w/v) in 1% acetic acid. After staining, unbound dye was removed by washing with 1% acetic acid and the plates were air-dried. Bound stain were subsequently solubilized with 10 mM tris(hydroxymethyl)aminomethane (Tris), and the absorbance was read on an automated plate reader at a wavelength of 540 nm. The above-mentioned assay enables determination of the drug concentration needed to inhibit cell growth by 50% (IC_{50}).

Sample preparation and 2D gel electrophoresis

Whole protein extracts were obtained from A2780/S cells and from A2780/S cells treated with Auoxo6 and auranofin. Briefly, the cells were seeded in tissue-culture plates at 5×10^4 cells/mL (total volume 30 mL) and incubated overnight, then exposed to concentrations of the study compounds equal to 72-h-exposure IC_{50} values for 24 h. At the end of the incubation the cells were washed with phosphate-buffered saline, then were scraped in RIPA buffer [50 mM Tris–HCl pH 7.0, 1% NP-40, 150 mM NaCl, 2 mM ethylene glycol bis(2-aminoethyl ether)tetraacetic acid, 100 mM NaF] containing a cocktail of protease inhibitors (Sigma). The cells were sonicated (10 s) and protein extracts were clarified by centrifugation at 8,000*g* for 10 min. Proteins were precipitated following a chloroform/methanol protocol [32] and the pellet was resuspended in 8 M urea, 4% 3-[(3-cholamidopropyl) dimethylammonio]propanesulfonic acid (CHAPS), and 20 mM dithiothreitol (DTT). Three independent experiments were performed and each sample was run in triplicate to assess biological and analytical variation. Isoelectric focusing (first dimension) was carried out on nonlinear wide-range immobilized pH gradients (IPGs; pH 3.0–10; 18-cm-long IPG strips; GE Healthcare, Uppsala,

Sweden) and achieved using an EttanTM IPGphor^{TM} system (GE Healthcare, Uppsala, Sweden). Analytical-run IPG strips were rehydrated with 60 μg of total proteins in 350 μL of lysis buffer and 0.2% carrier ampholyte for 1 h at 0 V and for 8 h at 30 V, at 20 °C. The strips were focused at 20 °C according to the following electrical conditions: 200 V for 1 h, from 300 to 3,500 V in 30 min, 3,500 V for 3 h, from 3,500 to 8,000 V in 30 min, and 8,000 V until a total of 80,000 V/h was reached. For preparative gels, 18-cm IPG strips (pH 3–10 NL) were rehydrated overnight for 20 h at room temperature in 350 μL of rehydration buffer containing 8 M urea, 2% w/v CHAPS, 0.5% DTT, and 0.5% IPG buffer with the same pH range as the Immobiline DryStrips and a trace of bromophenol blue. Rehydrated strips were rinsed in double-distilled water to remove urea crystals. Samples (up to 1 mg) were cup-loaded near the anode of the IPG strips using an Ettan IPGphor cup-loading manifold (GE Healthcare) according to the manufacturer's protocol.

After focusing, analytical and preparative IPG strips were equilibrated for 12 min in 6 M urea, 30% glycerol, 2% sodium dodecyl sulfate, 2% DTT in 0.05 M Tris–HCl buffer, pH 6.8, and subsequently for 5 min in the same urea/sodium dodecyl sulfate/Tris–HCl buffer solution where DTT was substituted with 2.5% iodoacetamide. The second dimension was carried out on 9–16% polyacrylamide linear gradient gels (18 cm × 20 cm × 1.5 mm) at 10 °C and 40 mA per gel constant current until the dye front reached the bottom of the gel. Analytical gels were stained with ammoniacal silver nitrate as previously described [33]; MS-preparative gels were stained with colloidal Coomassie [34].

Image analysis and statistics

Images of the gels were acquired with an Epson expression 1680 PRO scanner. For each condition, three biological replicates were performed and only the spots present in all the replicates were taken into consideration for subsequent analysis. Computer-aided 2D image analysis was carried out using ImageMaster 2D Platinum version 6.0 (GE Healthcare). The relative spot volume calculated as $\%V$ ($V_{\text{single spot}}/V_{\text{total spots}}$, where V is the integration of the optical density over the spot area) was used for quantitative analysis io decrease experimental errors. The normalized intensity of the spots on replicate 2D gels was averaged and the standard deviation was calculated. The mean values were compared among the three different conditions (control, auranofin-treated cells, and Auoxo6-treated cells) by analysis of variance followed by Tukey's post hoc multiple comparisons using the Graphpad Prism4 program. $P < 0.05$ was considered statistically significant.

Protein identification by mass spectrometry

Protein identification was carried out by peptide mass fingerprinting on an Ettan matrix-assisted laser desorption/ionization (MALDI) time of flight (TOF) Pro mass spectrometer (Amersham Biosciences), as previously described [35, 36]. Electrophoretic spots, visualized by a colloidal Coomassie staining protocol, were manually excised, destained, and acetonitrile-dehydratated. Successively, they were rehydratated in trypsin solution, and in-gel protein digestion was performed by an overnight incubation at 37 °C. From each excised spot, 0.75 μL of recovered digested peptides was prepared for MALDI-TOF MS by spotting them onto the MALDI target, allowing them to dry, and then mixing them with 0.75 μL of matrix solution [saturated solution of α-cyano-4-hydroxycinnamic acid in 50% (v/v) acetonitrile and 0.5% (v/v) trifluoroacetic acid]. After application of the matrix to the dried sample and drying, tryptic peptide masses were acquired. Mass-fingerprinting searching was carried out in the NCBInr and Swiss-Prot databases using Mascot (Matrix Science, London, UK, http://www.matrixscience.com). Protein identification was achieved on the basis of corresponding experimental and theoretical peptide-fingerprinting patterns. A mass tolerance of 100 ppm was allowed and only one missed cleavage site accepted. Alkylation of cysteine by carbamidomethylation was assumed as a fixed modification, whereas oxidation of methionine was considered a possible modification. The criteria used to accept identifications included the extent of sequence coverage, the number of matched peptides, and a probabilistic score, as reported in Table 2.

Tryptic digests that did not produce MALDI-TOF unambiguous identifications were subsequently acidified with 2 μL of a 1% trifluoroacetic acid solution, and then subjected to electrospray ionization (ESI)–ion trap MS/MS peptide sequencing using an LCQ DECA ion trap mass spectrometer (Thermo Finnigan, San Jose, CA, USA). With use of ZIP-TIPTM pipette tips for sample preparation (Millipore, Billerica, MA, USA), previously equilibrated in 50% acetonitrile solution and abundantly washed in 0.1% trifluoroacetic acid, acidified samples were enriched. Tryptic peptide elution from the ZIP-TIPTM matrix was achieved with a 70% methanol and 0.5% formic acid solution, and 3 μL of such concentrated sample solutions was then loaded in the nanospray needle. MS/MS database searching was performed by TurboSEQUEST (Thermo) and Mascot MS/MS ion search software (http://www.matrixscience.com) in the Swiss-Prot/TrEMBL or NCBInr databases. The following criteria were applied: MS accuracy ±1.2 Da, MS/MS mass accuracy ±0.6 Da, peptide precursor charge 2+, monoisotopic experimental mass values, trypsin digestion with one allowed missed cleavage,

fixed carbamidomethylation of cysteine, and variable oxidation of methionine.

Results

Antiproliferative effects of the chosen gold drugs toward A2780 cells

At first, the cytotoxic effects of auranofin on A2780 human ovarian carcinoma cells, either sensitive (A2780/S) or resistant (A2780/R) to cisplatin, were measured according to standard methods. On the ground of the SRB assay results, IC_{50} values of 0.5 and 0.3 μM were determined for auranofin on the sensitive and resistant cell lines, respectively, after 72-h drug exposure. In turn, the measured IC_{50} values for Auoxo6 were found to be perfectly consistent with those previously reported by Casini et al. [5] (1.8 and 4.9 μM for A2780/S and A2780/R, respectively). We also observed that very limited cell death was evident, for both compounds, at 24 h, this rendering a classic proteomic approach well feasible. Remarkably, the IC_{50} values obtained with auranofin and Auoxo6 closely match those recently determined for the same compounds on a 36 cell line panel [37].

Proteomic profiles of control and gold-treated cancer cells

To investigate in detail the mechanisms of cell death induced by these gold drugs, protein profiles of control, Auoxo6-treated, and auranofin-treated A2780 cells were studied by comparative proteomic analysis. A2780/S cells were treated, for 24 h, with auranofin and Auoxo6, at their 72-h-exposure IC_{50} concentrations (0.5 and 1.8 μM, respectively), and protein extracts were subsequently prepared, as described in "Materials and methods." Then, proteins were separated by 2D gel electrophoresis and the resulting silver-stained gels were analyzed using the ImageMaster 2D Platinum version 6.0. Representative 2D silver-stained gels for control, Auoxo6–treated, and auranofin-treated A2780/S cells are shown in Fig. 2. An average of about 1,300 protein spots was separated on the gels. To obtain statistically significant results, each protein sample was run in triplicate. The box highlights a major area where significant and consistent alterations of protein

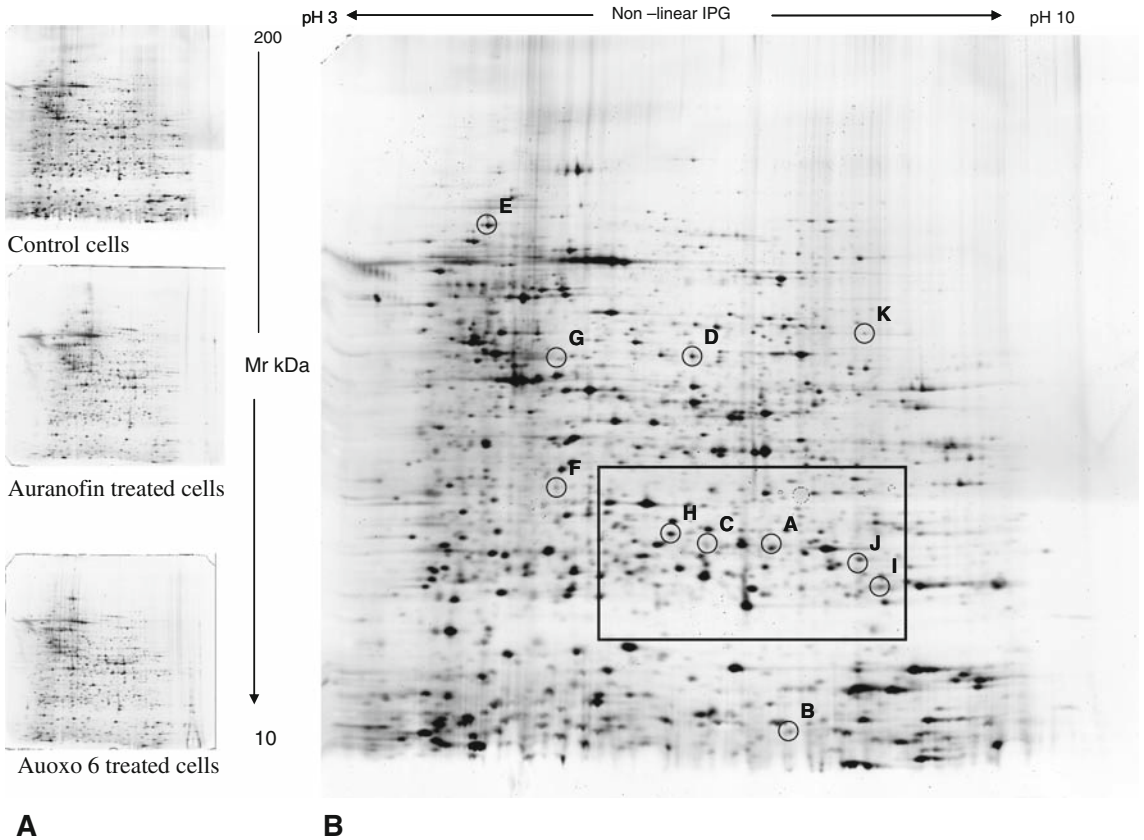

Fig. 2 **a** Representative 2D gel images for control cells, auranofin-treated cells, and Auoxo6-treated cells. **b** Representative gel image of A2780 control cells. The *box* highlights a major area where significant and consistent alterations of protein expression were identified *Circles* and *letters* indicate differentially expressed proteins

expression were identified. Circles and letters indicate differentially expressed proteins as emerged from comparative gel analysis.

Remarkably, auranofin and Auoxo6 treatments just caused very modest perturbations of the protein expression profiles. Indeed, only a very limited number of proteins, of the more than 1,300 monitored, showed appreciable downregulation or upregulation. Comparative computer analysis highlighted 11 meaningful variations between treated cells and control cells. Proteins with at least a 1.5-fold ($P < 0.05$) change in their expression level were considered as "changed" and were selected for further identification by MS. The locations of these protein spots are marked with capital letters in the representative gel shown in Fig. 2. The histograms in Fig. 3 illustrate the variation of protein expression for both drug treatments in comparison with untreated cells. As is evident from inspection of the histograms, three spots (spots F, G, and I) manifest a pronounced upregulation in both treated cells in comparison with the control; in contrast, three spots (spots A, B, and C) show a downregulation in both drug treatments. Finally four spots (spots D, E, H, and J) show a significant variation only when cells were treated with auranofin.

In Table 1 the quantitative data and the statistical analyses for the protein spots whose intensity levels significantly differed among A2780/S control cells and auranofin- or Auoxo6-treated cells are reported. A total of eight spots were successfully identified by MS.

Identification of differentially expressed proteins in gold-treated cells

Table 2 summarizes the parameters obtained from database-matching for protein identification, including protein name, NCBI database access number, sequence coverage, Mascot score, peptide matched, theoretical and experimental mass, and pI. In Fig. 4 an enlargement of spots corresponding to the identified differentially expressed proteins is shown with the corresponding changes in expression rate. Among the proteins that we identified, by MS, as upregulated in both auranofin- and Auoxo6-treated cells are ezrin (spot G), associated with the cytoskeleton [38], peroxiredoxin 1 (spot I), a peroxidase with a high antioxidant efficiency implicated in regulating proliferation [39], differentiation, and apoptosis, and fragments of the heterogeneous nuclear ribonucleoprotein (spot F), which provides the substrate for the processing events that precursor messenger RNA undergoes before becoming functional [40]. This protein was also identified in spot A corresponding to the full protein. Downregulation of histidine triad nucleotide-binding protein 1 (Hint1; spot B), an enzyme able to hydrolyze adenosine 5′-monophosphoramidate substrates [41], of oeroxiredoxin 6 (spot H), and of 3-hydroxyacyl-CoA dehydrogenase (spot J) functioning in mitochondrial transfer RNA maturation, were also observed [42].

Discussion

A2780 proteome responses to auranofin and Auoxo6 treatments

A classic proteomic approach, relying on 2D gel electrophoresis coupled with MS, was implemented here to identify altered proteins in the A2780/S human tumor cell line, in response to Auoxo6 and auranofin treatments. A total of 11 differentially expressed protein spots were detected in both cell treatments. Eight of these spots were successfully identified by MS. Not all spots could be identified because of the relatively low protein concentrations and of the sensitivity limitations of MS. Of the eight

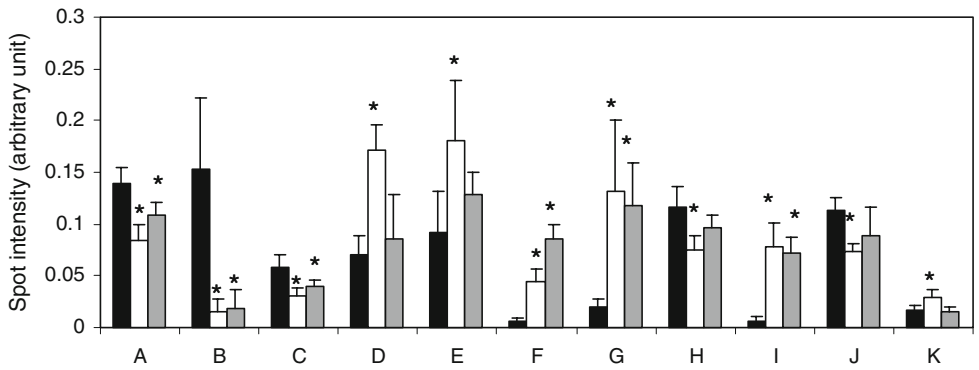

Fig. 3 Relative protein expression changes of auranofin-treated (*white bars*) and Auoxo6-treated (*gray bars*) cells versus control cells (*black*). *Bars* represent the mean ± the standard deviation of spots' volume percentage from three different experiments. *Asterisks* indicate that the difference is statistically significant $P < 0.05$. The volume percentage is calculated as $V_{\text{single spot}}/V_{\text{total spots}}$ (V is the integration of the optical density over the spot area)

Table 1 Quantitative data and statistical analyses of protein spots whose intensity levels significantly differed among A2780 control cells and auranofin- and Auoxo6-treated cells

Spot	Spot intensity (arbitrary unit)			ANOVA	Tukey's post hoc multiple comparisons		
	A2780 control cells	A2780 + auranofin	A2780 + Auoxo6		Control versus auranofin	Control versus Auoxo6	Auranofin versus Auoxo6
A	0.1392 ± 0.0148	0.0842 ± 0.0149	0.109 ± 0.0119	$P = 0.0012$	$P < 0.001$	$P < 0.05$	NS
B	0.1536 ± 0.0689	0.015241 ± 0.01236	0.017678 ± 0.018913	$P = 0.002$	$P < 0.01$	$P < 0.01$	NS
C	0.0584 ± 0.0115	0.03104 ± 0.0074	0.04054 ± 0.0048	$P = 0.0038$	$P < 0.01$	$P < 0.05$	NS
D	0.0706 ± 0.017626	0.17162 ± 0.0249	0.08515 ± 0.04376	$P = 0.0025$	*$P < 0.01$*	NS	P < 0.01
E	0.0927 ± 0.0396	0.1817 ± 0.0574	0.129 ± 0.0215	$P = 0.044$	*$P < 0.05$*	NS	NS
F	0.0063 ± 0.031	0.0443023 ± 0.012644	0.0852521 ± 0.0147189	$P < 0.0001$	$P < 0.01$	$P < 0.001$	$P < 0.01$
G	0.0195 ± 0.0083	0.1312 ± 0.0694	0.1184 ± 0.0413	$P = 0.0159$	$P < 0.05$	$P < 0.05$	NS
H	0.1157 ± 0.0120	0.075 ± 0.0134	0.0971 ± 0.0109	$P = 0.0139$	$P < 0.05$	NS	NS
I	0.0059 ± 0.0041	0.0779 ± 0.0224	0.0715 ± 0.0163	$P = 0.036$	$P < 0.05$	$P < 0.05$	NS
J	0.1133 ± 0.0122	0.0728 ± 0.0079	0.089469 ± 0.0265	$P = 0.028$	P < 0.05	NS	NS
K	0.0164 ± 0.0043	0.0293 ± 0.0073	0.0148 ± 0.005	$P = 0.0112$	$P < 0.05$	NS	P < 0.05

The mean values of individual parameters were compared among the three different conditions by analysis of variance (*ANOVA*) followed by Tukey's post hoc multiple comparisons using the GraphPad Prism4 program. $P < 0.05$ was considered statistically significant

NS not significant

Table 2 Matrix-assisted laser desorption/ionization time of flight (*MALDI-TOF*) mass spectrometry (*MS*) and MS/MS analyses of proteins whose levels significantly differed among control and treated cells

Spot	Protein identity	Accession no.	MALDI-TOF MS			MS/MS peptide sequence	Theoretical pI/molecular mass (kDa)	Experimental pI/molecular mass (kDa)[c]
			Score[a]	Coverage (%)[b]	No. of matched masses			
A	Heterogeneous nuclear ribonucleoprotein	P31943	101	26	8		5.89/49.5	5.7/26.8
B	Histidine triad nucleotide-binding protein 1	P49773	129	71	7		6.43/13.9	6.4/16.1
C	Triosephosphate isomerase + high-mobility group protein B1	P60174 + P09429	120 76	51% 27%	9 8	TATPQQAQEVHEK VPADTEVVCAPPTAYIDFAR + GEHPGLSIGDVAK	6.45/26.9 + 5.62/25.0	5.3/26.68 + 5.3/26.68
F	Heterogeneous nuclear ribonucleoprotein	P31943	107	28	7		5.89/49.5	5.4/30.9
G	Ezrin	P15311	72	13	7		5.94/69.5	5.4/46.5
H	Peroxiredoxin 6	P30041	66	22	5	LPFPIIDDR	6.00/25.1	6.2/27.1
I	Peroxiredoxin 1	Q06830	90	32	5	TIAQDYGVLK	8.27/22.3	7.9/20.4
J	3-Hydroxyacyl-CoA dehydrogenase type 2	Q99714	93	24	5	GLVAVITGGASGLGLATAER	7.87/27.1	7.7/25.9

[a] MS matching score greater than 65 was required for a significant MS hit

[b] Sequence coverage = (number of the identified residues/total number of amino acid residues in the protein sequence) × 100%

[c] Based on the calculation using ImageMaster 2D Platinum

identified proteins, six were altered in both cell treatments; at variance, two proteins showed a significant change in their expression levels only after auranofin treatment. It is noteworthy that both treatments, though causing extensive cell death at 72 h, induce very limited changes in the proteome at 24 h. Such a situation is markedly different from that found for cisplatin and for gold(III) porphyrin 1a in previous studies [11, 19], where far more pronounced and diffuse proteome alterations were detected, after 24 h. Conversely, the fact that most affected proteins are in

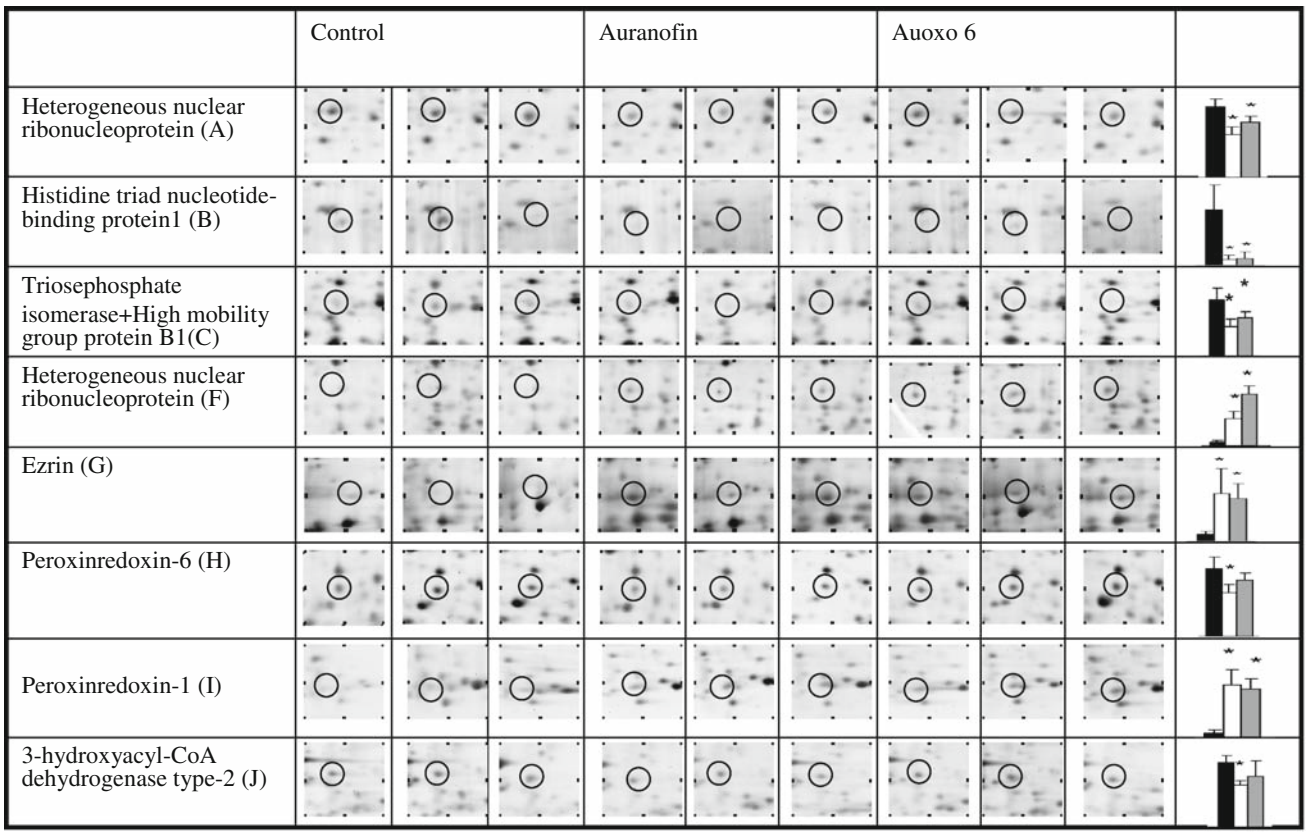

Fig. 4 Magnified regions of triplicate 2D gel images of spots corresponding to the identified proteins. Spots of interest are indicated with *circles*, with the corresponding protein names given on the *left*. In the column on the *right* the relative histograms are reported

common between the two treatments is highly suggestive of an identical (or at least very similar) effect of both Auoxo6 and auranofin against this cancer cell model. Remarkably, the affected proteins participate in a variety of cellular processes, such as cell structural organization, defense against oxidative stress, transcription, translation, and metabolism. More details on the functional roles of the affected proteins are given next.

Functional roles of the identified proteins

Morphological changes accompanied by cytoskeleton arrangement are considered as an hallmark of apoptosis [43]; in the present study, according to the 2D electrophoresis maps and MS/MS analysis, we observed an increase in the expression level of ezrin, a cytoskeleton regulatory protein involved in cellular events such as proliferation, cell migration, and apoptosis [44–46].

We also observed, upon Auoxo6 or auranofin treatment, an increase in the fragmentation of the heterogeneous nuclear ribonucleoprotein H; furthermore, we identified a downregulation in the expression of the complete protein. This protein is implicated in several steps of the precursor messenger RNA processing and in cellular differentiation [47]. Its overexpression was observed in primary carcinomas and metastases [48]; a downregulation of the protein and an increase of its fragmentation could be the result of drug treatments leading to the inhibition of cell proliferation and colony formation. Moreover, the overexpression of heterogeneous nuclear ribonucleoprotein H leads to production in HeLa cells of a proapoptotic alternative splice variant of Bcl-x [Blc-x(S)] [49]. At the time point of the Auoxo6 and auranofin treatments studied, no increased apoptosis was observed. We observed that apoptosis occurs at a later time point and that the increase of heterogeneous nuclear ribonucleoprotein H levels just precedes this process [50].

In the current study we found a reduced expression of Hint1. It is a member of the evolutionarily conserved family of histidine triad proteins that acts as a haploinsufficient tumor suppressor; the molecular mechanisms for the tumor-suppressing activity are poorly defined. Consistent with a tumor suppressor function, in the human non-small-cell lung cancer cell line NCI-H522, an alteration in Hint1 expression was observed and reintroduction of Hint1 resulted in cell growth inhibition and reduced tumorigenicity [51]. Reduced or lost expression of tumor suppressor proteins is often associated with impaired

induction of apoptosis. Hint1 is involved in the regulation of apoptotic pathways by inducing an upregulation of p53 expression coinciding with an upregulation of the proapoptotic factor Bax and a concomitant downregulation of the apoptosis inhibitor Bcl-2. Hint1 appears to modulate transcriptional regulation, cell cycle control, and induction of apoptosis [52].

Also, we observed an increased expression pattern of peroxiredoxin 1 in response to both treatments. In contrast, we found a reduced expression of peroxiredoxin 6 as a result of auranofin treatment. Peroxiredoxins are increased in a number of cancers, including lung cancer [53], and have been correlated to radioresistance and resistance to cisplatin [54] The peroxiredoxins also influence a variety of cellular processes that are sensitive to reactive oxygen species and play a role in signal transduction and gene expression related to alteration in cellular reactive oxygen species levels [55]. In many cases increased peroxiredoxin expression correlated to chemoresistance; our results suggest that treatment with both drugs, modifying the expression of peroxiredoxin, disrupts total cellular redox homeostasis and induces apoptosis. Peroxiredoxin II could be the focus of new drugs for use in the treatment of cancer. It was previously reported [56] that inactivation of the stress-activated protein peroxiredoxin constitutes a promising approach to the development of improved cancer treatments, and that inhibitors of peroxiredoxin represent very good anticancer drug candidates, especially in the role of chemosensitizers or radiosensitizers.

Inferences on the molecular mechanisms of Auoxo6 and auranofin

The results reported above contain some important implications concerning the possible mechanism of action of Auoxo6 and auranofin, observed from the "point of view" of the cell. Previous studies had highlighted that Auoxo6, a binuclear gold(III) compound developed in our laboratories, manifests remarkable cytotoxic properties, with IC_{50} values falling in the low micromolar range [5]. Moreover, Auoxo6 is characterized by a rather pronounced selectivity in its cytotoxic properties toward a large panel of 36 cell lines as reported earlier [37]. Owing to the still appreciable oxidizing properties of the gold(III) center, it can be assumed that Auoxo6 may undergo facile reduction and cleavage, thus being a source of gold(I) species. Indeed, ESI-MS interaction studies with model proteins strongly supported this view [57].

More extensive and detailed knowledge is available on auranofin and its biochemical and cellular effects. Indeed, auranofin is a drug in clinical use, since 1978, for the treatment of rheumatoid arthritis, and a large amount of documentation now exists on it. In particular, it was shown that this compound is strongly cytotoxic and propapoptotic in vitro and that apoptosis is probably mediated by a direct mitochondrial mechanism. Strong inhibition of thioredoxin reductase by auranofin was demonstrated as well in a number of studies [12].

Remarkably, the present proteomic investigation revealed that both assayed gold compounds, though being highly cytotoxic (at 72 h), produce rather limited changes in the protein expression patterns at 24 h, implying that cell damage, at least in the early phases, is quite selective and limited. Also, it is of interest to stress that the patterns of induced protein alterations are very similar in the two cases, pointing out that the modes of action of these two compounds may be nearly identical. This observation most likely implies that Auoxo6, in the cellular milieu, is reduced to a gold(I) species and that the mode of action of the latter species closely matches that of auranofin. It was previously proposed that strong inhibition of thioredoxin reductase might constitute a peculiar feature of the cytotoxic mechanism of auranofin and of several other gold-based compounds: Thus, it is well conceivable that the gold(I) species resulting from Auoxo6 reduction might act as a strong inhibitor of thioredoxin reductase and thus cause its proapoptotic effects.

The few proteins whose expression is affected by these gold drugs deserve some final comments. The increase in ezrin expression might be considered as an initial sign of apoptosis as the apoptotic process is known to involve a large rearrangement of the cytoskeleton and of cell morphology. In turn, the observed alterations in peroxiredoxins 1 and 6, which are nicely consistent with previous observations on the cellular effects of a gold(III) porphyrin, are strongly suggestive of a intense cellular response to drug-induced oxidative stress. Moreover, the marked increase in heterogeneous ribonucleoprotein H is indicative of caspase 3 activation.

It may be hypothesized that these gold drugs elicit a significant intracellular oxidative stress that cells attempt to counteract during the early phases of treatment by activation of intrinsic defense mechanisms; failure to counteract oxidative stress will eventually cause apoptotic cell death. Additional time course proteomic analyses are being planned to better identify and characterize the proposed sequence of intracellular events.

Concluding remarks

The results of this proteomic study point out that the mode of action of Auoxo6 is very similar to that of auranofin, strongly suggesting that Auoxo6 reduction to a gold(I) species takes place within the biological milieu. Quite unexpectedly, the perturbations in the protein expression

patterns induced by both gold compounds, after 24-h incubation, are limited and selective, far less pronounced than those caused by other metallodrugs previously investigated. Some of the affected proteins are primarily involved in the intracellular redox homeostasis, implying that cell damage is probably the consequence of severe oxidative stress; pairwise, two proteins that are biomarkers of apoptosis were found to be greatly perturbed. The value of novel proteomic approaches to decipher the complex biochemical and cellular mechanisms of anticancer metallodrugs is further supported by the present investigation.

References

1. Bruijnincx PC, Sadler PJ (2008) Curr Opin Chem Biol 12:197
2. Zhang CX, Lippard SJ (2003) Curr Opin Chem Biol 7:481
3. Casini A, Hartinger C, Gabbiani C, Mini E, Dyson PJ, Keppler BK, Messori L (2008) J Inorg Biochem 102:564
4. Nobili S, Mini E, Landini I, Gabbiani C, Casini A, Messori L (2009) Med Res Rev (in press)
5. Casini A, Cinellu MA, Minghetti G, Gabbiani C, Coronnello M, Mini E, Messori L (2006) J Med Chem 49:5524–5531
6. Gabbiani C, Casini A, Messori L, Guerri A, Cinellu MA, Minghetti G, Corsini M, Rosani C, Zanello P, Arca M (2008) Inorg Chem 47:2368–2379
7. Kean WF, Hart L, Buchannan WW (1997) Br J Rheumatol 36:560–572
8. Gandin V, Fernandes AP, Rigobello MP, Dani B, Sorrentino F, Tisato F, Björnstedt M, Bindoli A, Sturaro A, Rella R, Marzano C (2010) Biochem Pharmacol 79:90–101
9. Marzano C, Gandin V, Folda A, Scutari G, Bindoli A, Rigobello MP (2007) Free Radic Biol Med 42:872–881
10. Coronnello M, Mini E, Caciagli B, Cinellu MA, Bindoli A, Gabbiani C, Messori L (2005) J Med Chem 48:6761
11. Wang Y, He QY, Sun RWY, Che CM, Chiu JF (2005) Cancer Res 65:11553–11564
12. Bindoli A, Rigobello MP, Scutari G, Gabbiani C, Casini A, Messori L (2009) Coord Chem Rev 253:1692–1707
13. Rigobello MP, Scutari G, Boscolo R, Bindoli A (2002) Br J Pharmacol 136:1162
14. He QY, Chiu JF (2003) J Cell Biochem 89:868–886
15. Stoughton RB, Friend SH (2005) Nat Rev Drug Discov 4:345–350
16. Wang Y, Chiu JF (2008) Met Based Drugs 2008:716329
17. Yim EK, Lee KH, Kim CJ, Park JS (2006) Int J Gynecol Cancer 16:690–697
18. Yao Y, Jia XY, Tian HY, Jiang YX, Xu GJ, Qian QJ, Zhao FK (2009) Biochim Biophys Acta 1794:1433–1440
19. Che CM, Sun RWY, Yu WY, Ko CB, Zhu N, Sun H (2003) Chem Commun 14:1718–1719
20. Wang Y, He QY, Che CM, Chiu JF (2006) Proteomics 6:131–142
21. Wang Y, He QY, Sun RWY, Che CM, Chiu JF (2007) Eur J Pharmacol 554:113–122
22. Mounicou S, Szpunar J, Lobinski R (2009) Chem Soc Rev 38:1119–1138
23. Shi W, Chance (2008) Cell Mol Life Sci 65:3040–3048
24. Garcia JS, Magalhães CS, Arruda MA (2006) Talanta 69:1–15
25. Will J, Wolters DA, Sheldrick WS (2008) Chem Med Chem 3:1696–1707
26. Allardyce CS, Dyson PJ, Abou-Shakra FR, Birtwistle H, Coffey J (2001) Chem Commun 2:2708–2709
27. Will J, Sheldrick WS, Wolters D (2007) J Biol Inorg Chem 13:421–434
28. Khalaila I, Bergamo A, Bussy F, Sava G, Dyson PJ (2006) Int J Oncol 29:261–268
29. Becker JS, Mounicou S, Zoriy MV, Becker JS, Lobinski R (2008) Talanta 76:1183–1188
30. Cinellu MA, Minghetti G, Pinna MV, Stoccoro S, Zucca A, Manassero M, Sansoni MJ (1998) Chem Soc Dalton Trans 1735–1741
31. Skehan P et al (1990) J Natl Cancer Inst 82:1107–1112
32. Wessel D, Flügge A (1984) Anal Biochem 138:141–143
33. Hochstrasser DF, Patchornik A, Merril CR (1988) Anal Biochem 173:412–423
34. Neuhoff V, Arold N, Taube D, Ehrhardt W (1988) Electrophoresis 9:255–262
35. Hellman U, Wernstedt C, Gonez J, Heldin CH (1995) Anal Biochem 224:451–455
36. Soskic V, Gorlach M, Poznanovic S, Boehmer FD, Godovac-Zimmermann J (1999) Biochemistry 38:1757–1764
37. Casini A, Kelter G, Gabbiani C, Cinellu MA, Minghetti G, Fregona D, Fiebig HH, Messori L (2009) J Biol Inorg Chem 14:1139–1149
38. Fiévet B, Louvard D, Arpin M (2007) Biochim Biophys Acta 1773:653–660
39. Karplus PA, Hall A (2007) Subcell Biochem 44:41–60
40. Krecic AM, Swanson (1999) Curr Opin Cell Biol 11:363–371
41. Brenner C, Bieganowski P, Pace HC, Huebner K (1999) J Cell Physiol 181:179–187
42. Yang SY, He XY, Schulz H (2005) FEBS J 272:4874–4883
43. Ndozangue-Touriguine O (2008) Biochem Pharmacol 76:11–18
44. Yao Yi, Xiao-Yuan Jia et al (2009) BBA Proteins Proteomics 1794:1433–1440
45. Orian-Rousseau V, Morrison H, Matzke A et al (2007) Mol Biol Cell 18:76–83
46. Lee YJ, Keng PC (2005) Mol Biotechnol 31:1–10
47. Honore B, Baandrup U (2004) Exp Cell Res 249:199–209
48. Rauch J, Ahlemann M et al (2004) Biochem Biophys Res Commun 323:156–162
49. Garneau D, Revil T et al (2005) J Biol Chem 280:22641–22650
50. Brockstedt E, Rickers A, Kostka S, Laubersheimer A, Dorken B, Wittmann-Liebold B, Bommert K, Otto A (1998) J Biol Chem 273:28057–28064
51. Yuan BZ, Jefferson AM, Popescu NC, Reynolds SH (2004) Neoplasia 6:412–419
52. Weiske J, Huber O (2006) J Biol Chem 281:27356–27366
53. Park JH, Kim YS, Lee HL, Shim JY et al (2006) Respirology 11:269–275
54. Chang JW, Jeon HB, Lee JH, Yoo JS et al (2001) Biochem Biophys Res Commun 289:507–512
55. Lim MJ, Chae HZ, Rhee SG, Yu DY et al (1998) Gene 216:197–205
56. Yo YD, Chung YM, Park JK, Ahn CM, Kim SK, Kim HJ (2002) Exp Mol Med 34:273–277
57. Casini A, Cinellu MA, Minghetti G, Gabbiani C, Coronnello M, Mini E, Messori L (2006) J Med Chem 49:5524–5531